

University of Nebraska - Lincoln

DigitalCommons@University of Nebraska - Lincoln

Virology Papers

Virology, Nebraska Center for

3-2012

***Paramecium bursaria* Chlorella Virus 1 Encodes a Polyamine Acetyltransferase**

Zachary Charlop-Powers

Mount Sinai School of Medicine, New York, Zachary.Charlop-Powers@mssm.edu

Jean Jakoncic

Brookhaven National Laboratory, jjakoncic@bnl.gov

James R. Gurnon

University of Nebraska-Lincoln, jgurnon2@unl.edu

James L. Van Etten

University of Nebraska-Lincoln, jvanetten1@unl.edu

Ming-Ming Zhou

Mount Sinai School of Medicine, New York, ming-ming.zhou@mssm.edu

Follow this and additional works at: <https://digitalcommons.unl.edu/virologypub>



Part of the [Virology Commons](#)

Charlop-Powers, Zachary; Jakoncic, Jean; Gurnon, James R.; Van Etten, James L.; and Zhou, Ming-Ming, "*Paramecium bursaria* Chlorella Virus 1 Encodes a Polyamine Acetyltransferase" (2012). *Virology Papers*. 221.

<https://digitalcommons.unl.edu/virologypub/221>

This Article is brought to you for free and open access by the Virology, Nebraska Center for at DigitalCommons@University of Nebraska - Lincoln. It has been accepted for inclusion in Virology Papers by an authorized administrator of DigitalCommons@University of Nebraska - Lincoln.

Paramecium bursaria Chlorella Virus 1 Encodes a Polyamine Acetyltransferase^{*[S]}

Received for publication, December 27, 2011, and in revised form, January 17, 2012
Published, JBC Papers in Press, January 25, 2012, DOI 10.1074/jbc.C111.337816

Zachary Charlop-Powers[‡], Jean Jakoncic[§], James R. Gurnon[¶],
James L. Van Etten[¶], and Ming-Ming Zhou^{‡1}

From the [‡]Department of Structural and Chemical Biology, Mount Sinai School of Medicine, New York, New York 10029, the [§]National Synchrotron Light Source, Brookhaven National Laboratory, Upton, New York 11973, and the [¶]Department of Plant Pathology and Nebraska Center for Virology, University of Nebraska, Lincoln, Nebraska 68583-0900

Background: PBCV-1 gene *a654l* encodes a protein with sequence similarity to GCN5 histone acetyltransferases.

Results: A crystal structure of A654L bound to coenzyme A reveals how A654L acetylates polyamines, not histone lysines.

Conclusion: A654L functions as a polyamine acetyltransferase.

Significance: As the first viral polyamine acetyltransferase, A654L has a possible role in host polyamine catabolism in viral replication.

Paramecium bursaria chlorella virus 1 (PBCV-1), a large DNA virus that infects green algae, encodes a histone H3 lysine 27-specific methyltransferase that functions in global transcriptional silencing of the host. PBCV-1 has another gene *a654l* that encodes a protein with sequence similarity to the GCN5 family histone acetyltransferases. In this study, we report a 1.5 Å crystal structure of PBCV-1 A654L in a complex with coenzyme A. The structure reveals a unique feature of A654L that precludes its acetylation of histone peptide substrates. We demonstrate that A654L, hence named viral polyamine acetyltransferase (vPAT), acetylates polyamines such as putrescine, spermidine, cadaverine, and homospermidine present in both PBCV-1 and its host through a reaction dependent upon a conserved glutamate 27. Our study suggests that as the first virally encoded polyamine acetyltransferase, vPAT plays a possible key role in the regulation of polyamine catabolism in the host during viral replication.

Post-translational modifications of DNA-packing histones provide an attractive mechanism for viral manipulation of the

^{*} This work was supported, in whole or in part, by National Institutes of Health Grants R01HG004508 and R01CA87658 (to M.-M. Z.) and NCRP P30RR31151 (to J. L. V. E.). This work was also supported by National Science Foundation EPSCoR EPS-1004094 (to J. L. V. E.).

^[S] This article contains supplemental Materials and Methods, Table 1, and Figs. 1–7.

The atomic coordinates and structure factors (code 3QB8) have been deposited in the Protein Data Bank, Research Collaboratory for Structural Bioinformatics, Rutgers University, New Brunswick, NJ (<http://www.rcsb.org/>).

¹ To whom correspondence should be addressed: 1425 Madison Ave., Box 1677, New York, NY 10029. Fax: 212-849-2456; E-mail: ming-ming.zhou@mssm.edu.

host genome as well as host immune response to viral infection (1, 2). To date, the best studied virus-encoded chromatin-modifying enzyme, vSET (viral SET domain protein), comes from the chlorella virus PBCV-1,² a DNA virus that consists of an ~330-kb genome and encodes about 400 proteins, among which are a number of other specialized proteins including the smallest functional potassium channel (3, 4); the enzymes involved in the complete biosynthetic pathway for the rare polyamine homospermidine (5, 6); as well as the enzymes for endoplasmic reticulum- and Golgi-independent protein glycosylation (7). Our recent studies have shown that vSET functions to specifically methylate histone H3 at lysine 27 with the functional consequence of silencing the host genome; in heterologous expression systems, vSET suppresses host transcription within 1 h (8, 9). In addition to histone lysine methylation, lysine acetylation also has strong regulatory capability on gene transcription in chromatin. Remarkably, the PBCV-1 genome has a gene, *a654l*, that encodes a protein with sequence similarity to the GCN5 family of histone acetyltransferases (HATs) that are known for their role in chromatin remodeling and gene transcriptional activation through hyperacetylation of histone lysines (10, 11). To understand the structure and function of A654L, in this study, we determined a 1.5 Å resolution crystal structure of A654L bound to CoA and discovered and performed structure-guided characterization of the acetyl transfer reaction of A654L with an unexpected class of substrates.

EXPERIMENTAL PROCEDURES

Protein Preparation—The *a654l* gene from the PBCV-1 viral genome was cloned into a pET-15b vector using PCR primers incorporating NdeI and BglII restriction sites. The N-terminal His₆-tagged fusion protein was expressed in *Escherichia coli* (strain BL21 DE3) cells by overnight induction at 18 °C using 0.4 mM isopropyl-1-thio-β-D-galactopyranoside. Cell pellets were washed and lysed using a Microfluidizer in an ice-cold lysis buffer of 100 mM NaCl, 1 mM EDTA, 10 mM DTT, and 0.5% Nonidet P-40. A654L protein was purified by nickel-nitrilotriacetic acid affinity column chromatography followed by size-exclusion chromatography on a Superdex 75 column. Overnight cleavage of the His₆ tag was followed by flow over a SOURCE Q ion exchange column into a final buffer of 20 mM Tris, pH 8.5, containing 200 mM NaCl.

Site-directed Mutagenesis—A654L point mutants were generated by pfu PCR amplification of wild-type DNA with mutation-containing primers designed by PrimerX. PCR mixtures were digested with DpnI and transformed into DH5α *E. coli* cells. The presence of appropriate mutations was verified by DNA sequencing.

Crystallization—To optimize protein solubility, we followed the protocol of Jancarik *et al.* (12) and found that A654L yielded

² The abbreviations used are: PBCV-1, *P. bursaria* chlorella virus 1; HAT, histone acetyltransferase; SAD, single anomalous dispersion; GNAT, GCN5-related *N*-acetyltransferase; TAPS, {[2-hydroxy-1,1-bis(hydroxymethyl)ethyl]amino}-1-propanesulfonic acid; vPAT, viral Polyamine Acetyltransferase; vSET, viral SET domain protein.

REPORT: Structure of a Viral Spermine Acetyltransferase

the most homogeneous light-scattering profile in Tris buffer of pH 8.5 containing 200 mM NaCl and 1 mM DTT, which was then used as our standard buffer. For initial crystallization trials of A654L, we used 96-well sitting-drop Intelli-Plates (Hampton Research) and screened against the Hampton Crystal, Index, and Wizard screening conditions. Mother liquor of 1 μ l was mixed with 1 μ l of A654L immediately prior to the addition of 5 molar eq acetyl-CoA. Final protein concentration in the drops was 9 mg/ml. Optimization of pH, salt, and cryoprotectant yielded crystals in a buffer of 0.9 M sodium citrate, 100 mM glycine-NaOH, 100 mM imidazole, 150 mM NaCl, and 15% glycerol. Data were collected with the X6A beam-line at the Brookhaven National Laboratory. Diffraction data to 1.5 Å was collected from these crystals. Absent a highly homologous structure, we also collected SAD data using sulfur as the anomalous diffractor. Sulfur-SAD data were collected at a 1.77 Å wavelength for 1,000° of rotation at a final resolution of 1.9 Å. Diffraction data were scaled and integrated using HKL2000. Data were processed using the Phenix suite of crystallographic tools (13). Anomalous data from the Sulfur-SAD were input into AutoSolve, with instructions to use the SAD data to provide initial phase information and merge the native 1.5 Å dataset for refinement. Further refinement was iterated between Coot (14), PyMOL, and Phenix. Ambiguous density in the binding pocket led us to try co-crystallization of A654L with CoA, as well as both CoA and spermine. Crystal conditions were those used above, but the structure was solved using molecular replacement from our original structure. The protein was crystallized in the presence of CoA and spermine, although electron density was visible only for CoA. X-ray data collection and refinement statistics are listed in Table 1.

Mass Spectrometry—To test for the presence of acetylated species using mass spectrometry, we set up 20- μ l HAT reactions with the following composition: 100 μ M Hepes buffer of pH 7.4, containing 100 μ M acetyl-CoA, 20 μ M histone peptide substrate, and 50 nM A654L or histone acetyltransferase 1 (HAT1) (gift from A. Plotnikov). Reactions were incubated for 30 min at room temperature. Samples were diluted to 50 μ l with water and submitted for HPLC-MS analysis with a loading volume of 5 μ l. Raw data were exported as a text file, and traces were generated using mMass (15). Expected mass spectrometry peaks were monitored to confirm reactions. Reactions using spermine and spermidine as substrates also used 20 μ M concentrations.

Enzyme Kinetics Study Using Fluorescent Assay—To characterize the enzyme kinetics of A654L, we used a fluorescent assay that uses a thiol-reactive dye, 7-diethylamino-3-(4'-maleimidylphenyl)-4-methylcoumarin, to monitor acetylation reaction progression. Following the protocol reported by Treivel *et al.* (16), we set up 50- μ l reactions with buffer, substrate, acetyl-CoA, and the enzyme. Reactions were stopped with 50 μ l of ice-cold propanol after 2 min. 100 μ l of 25 μ M 7-diethylamino-3-(4'-maleimidylphenyl)-4-methylcoumarin was added, allowed to incubate for 10 min in the dark, and then measured for fluorescent absorption/emission at 390/450 nm using the Tecan Safire plate reader (Tecan) with a gain setting of 45. Data for all experiments were collected in triplicate, and background signal, which constitutes the reaction mixture without enzyme, was subtracted. Raw data were imported and processed in

TABLE 1
Crystallographic data collection and refinement statistics

	Sulfur-SAD	Native
Data collection		
Space group	P31	P31
Cell dimensions		
<i>a</i> , <i>b</i> , <i>c</i> (Å)	65.4, 65.4, 112.6	65.4, 65.4, 112.6
α , β , γ (°)	90, 90, 120	90, 90, 120
Resolution (Å)	30-1.9	28.2-1.36 (1.41-1.5)
Completeness (%) ^a	50 (33)	98.6 (85.9)
<i>R</i> _{sym} or <i>R</i> _{merge} (%) ^b	8 (50)	6 (37)
<i>I</i> / σ <i>I</i>	64.4 (8.7)	32.1 (3.6)
Redundancy	76.6 (7.7)	5.1-(4.9)
Refinement		
Resolution (Å)		28.3-1.5-(1.55-1.5)
No. of reflections		41,147 (405)
<i>R</i> _{work} / <i>R</i> _{free} (%) ^{c,d}		15.3/16.8
No. of atoms (protein, ligand/ion, water)		3,256/96/449
<i>B</i> -factors (protein, ligand/ion, water) (Å ²)		15.4/23.8/28.4
r.m.s. deviations ^e		
bond length (Å)/angle (°)		0.017/1.693

^a Numbers in parentheses refer to the highest resolution shell.

^b $R_{\text{merge}} = \sum |I - \langle I \rangle| / \sum I$, where *I* is the integrated intensity of a given intensity.

^c $R_{\text{work}} = \sum \|F_o\| - |F_c| / \sum \|F_o\|$.

^d *R*_{free} was calculated using 10% random data omitted from the refinement.

^e r.m.s., root mean square.

GraphPad Prism using the Michaelis-Menten parameters. Conversion from intensity to units of CoA was obtained by the use of a control plate consisting of a serial dilution of CoA. Data for all experiments were limited to the linear absorbance range. Acetyl-CoA for enzymatic reactions was pretreated with acetic anhydride before freezing aliquots of 6 mM. To study the enzyme kinetics of A654L for each of the polyamine substrates including spermine, spermidine, putrescine, cadaverine, and sym-homospermidine (kind gift of P. Woster), we set up triplicate serial dilutions of each polyamine ranging from 15 μ M to 3 mM. Reaction mixtures of 50 μ l contained polyamine, 50 μ M acetyl-CoA, and 50 μ M Tris buffer of pH 8. Reactions were initiated by adding 5 μ l of A654L for a final concentration of 50 nM. Absorbance data were converted to velocity, and Michaelis-Menten parameters were obtained using GraphPad Prism.

Profiling pH-dependent Enzyme Kinetics—The enzyme kinetics study was conducted as described above at pH 6.9–9.3 with increments of 0.3 pH units. HEPES buffer was used for pH 6.9–7.6, and TAPS buffer was used for pH 7.9–9.6. Data of $\log k_{\text{cat}}$ and $\log(k_{\text{cat}}/K_m)$ were plotted (supplemental Fig. 5) and fitted to the following equations: $\log k_{\text{cat}} = \log(k_{\text{max}}/(1 + [H^+]/K_1))$ and $\log k_{\text{cat}}/K_m = \log(k_{\text{max}}/(1 + [H^+]/K_1 + K_2/[H^+]))$, where *k*_{max} is the pH-independent plateau value, *K*₁ is the ionization constant for the acidic group, *K*₂ is the ionization constant for the basic group, and [H⁺] is the hydrogen ion concentration.

RESULTS AND DISCUSSION

The cloned full-length PBCV-1 A654L was purified to homogeneity as described under “Experimental Procedures.” Because we predicted acetyl-CoA would be a cofactor, we co-crystallized A654L in the presence of either acetyl-CoA or CoA and obtained crystals of the binary complex to a resolution of 1.5 Å (supplemental Fig. 1). Taking advantage of the 11 sulfur atoms in A654L, we obtained the phases of the A654L-CoA diffraction pattern by collecting a second anomalous dataset and refined the structure with the native dataset (Table 1). The

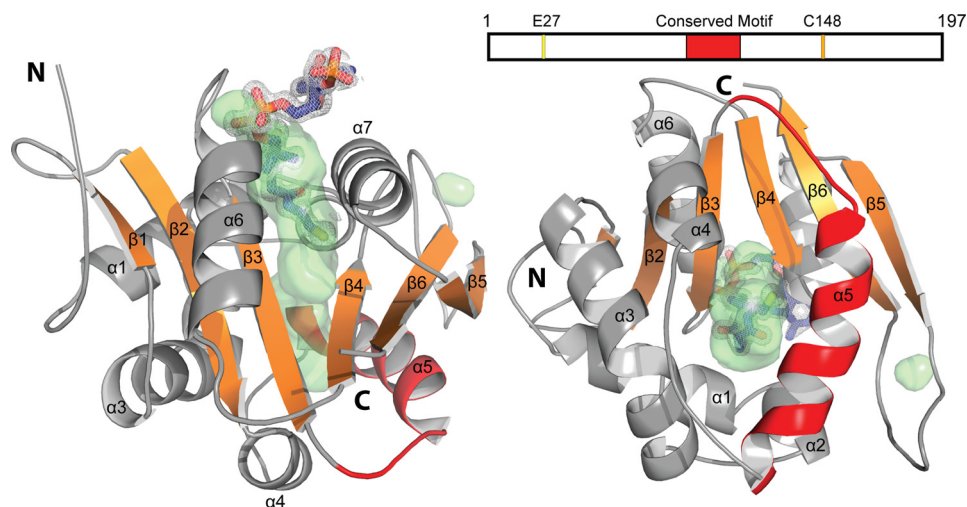


FIGURE 1. **Three-dimensional crystal structure of A654L encoded by virus PBCV-1.** A654L has a conserved GNAT fold characterized by the six-stranded β -sheet. Coenzyme A and the electron density map are shown along with the conserved motif (red) that distinguishes A654L from other GNAT structures. Access to the catalytic site can occur through a water-filled channel (green) that goes through the entire protein.

structure of A654L shows the canonical GNAT fold of a six-stranded β -sheet with interspersed helices (Fig. 1). The conserved acetyl-CoA binding features are present including the bulge between $\beta 3$ and $\beta 4$ that serves as the Ac-CoA-binding cavity; the short loop of Gly-121–Leu-124 below $\alpha 6$ comprises the conserved GXGX motif where the backbone amides form hydrogen bonds with CoA phosphates. The carbonyl oxygen of the CoA pantethine arm is also hydrogen-bonded to backbone amides of residues in $\beta 4$, and the amide of conserved asparagine, Asn-150, coordinates two CoA carbonyl oxygen atoms.

Although the A654L-CoA structure has conserved CoA binding features, it contains a secondary structural element comprising $\alpha 5$ and flanking residues that is incompatible with a peptide substrate (Fig. 1, red; supplemental Fig. 2). Superposition with the GCN5-H3 peptide complex structure (supplemental Fig. 3) shows that the conserved A654L insert is situated where an incoming substrate would sit. Instead of having an open substrate-binding cleft like the histone-acetylating GCN5, the catalytic site of A654L is completely enclosed within a tunnel running through the interior of the protein, which is visualized by the enclosed surface volume (Fig. 1, green). Furthermore, mapping of the electrostatic potential reveals that the channel is negatively charged (supplemental Fig. 4), suggesting an unbranched and positively charged substrate such as a polyamine. Subjecting the A654L structure to a Dali structure similarity search yielded several structures with unknown functions along with a polyamine acetyltransferase from *Bacillus subtilis* (Protein Data Bank (PDB): 1TIQ) with a moderate Dali Z-score (17) of 15.1, strengthening the likelihood that A654L might acetylate polyamines.

We investigated the acetyltransferase activity of A654L using a mass spectrometry method. In contrast to the well characterized human HAT1 (18), which effectively monoacetylates histone H4 peptide, A654L showed no acetyltransferase activity with peptides derived from histone 3 or 4 (Fig. 2a). However, A654L acetylated two common polyamines, spermine and spermidine, in a concentration-dependent manner (Fig. 2b). As PBCV-1 and its host, *Chlorella* NC64A, contain several poly-

amines including putrescine, spermidine, cadaverine, and homospermidine (5), we measured the catalytic activity of A654L against each of these substrates as well as the common mammalian polyamine spermine. Using a fluorescence assay that indirectly measures CoASH production, we discovered that A654L acetylates tetra-amines (spermine), triamines (spermidine and sym-homospermidine), as well as diamines (cadaverine and putrescine) (Fig. 2, b and c; also see supplemental Table 1). Although spermine is the preferred substrate, it was not previously detected in either the viral particle or *Chlorella* NC64A. Of the four polyamines detected in both the host and the virus, A654L prefers cadaverine 6-fold over the next polyamine, homospermidine. Given its acetyltransferase activity against polyamines, we gave A654L the name vPAT.

Structural analysis of the vPAT catalytic site suggests that either Cys-148 or Glu-27 may be important for catalysis that may proceed through one of two plausible mechanisms. Transfer of the acetyl group from acetyl-CoA to a substrate could occur either through an acetyl enzyme intermediate or by direct nucleophilic attack of an incoming polyamine on the acetyl group of the cofactor followed by formation of a tetrahedral intermediate and its conversion to the product of acetylated polyamine. The latter mechanism is assisted by a nearby residue that acts as a general base. Glu-27 is the only acidic residue that is close enough to the substrate at the active site (Fig. 2d).

We generated C148A and E27Q mutants to investigate the effects of the mutation on enzyme kinetics. The C148A mutant had no significant effect on k_{cat} , whereas the E27Q mutation resulted in a 26-fold reduction in k_{cat} and 126-fold reduction in k_{cat}/K_m . These results indicate that Glu-27 is likely a key residue for catalysis. Plotting $\log k_{cat}$ versus pH (supplemental Fig. 5) reveals pH dependence of the enzyme activity associated with two pK_a values of 7.12 and 9.37, likely representing ionizable groups involved in catalysis. The lower pK_a could be accounted for by Glu-27, whereas the higher pK_a might be a base such as Tyr-84, Tyr-79, or Tyr-76 that functions to donate a proton to the tetrahedral intermediate via a network of water molecules. It is worth noting that when one compares the vPAT sequences

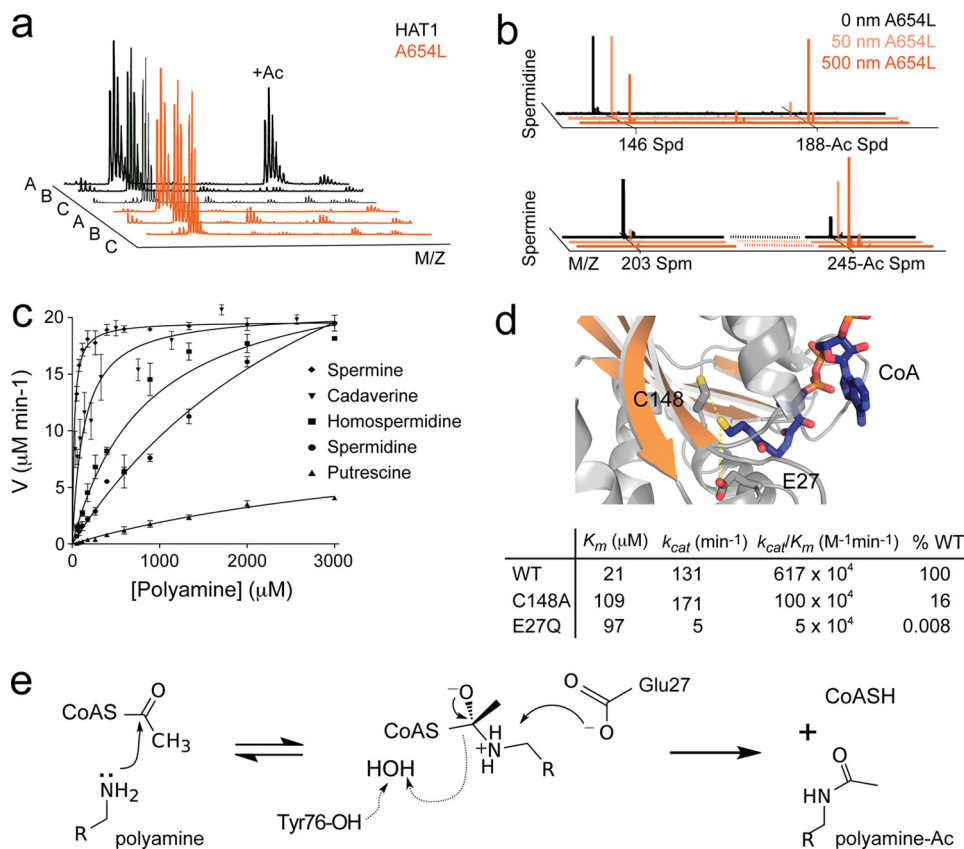


FIGURE 2. A654L is a polyamine acetyltransferase. *a*, HPLC-MS profiles depicting the acetyltransferase activity of human HAT1 and A654L for histone H3 or H4 peptide substrates (A, H4 of residues 1–22; B, H3 of residues 1–18; C, H3 of residues 1–13). *b*, mass spectrometry profiles of spermine and spermidine following incubation with A654L of 0, 50, or 500 nm. *c*, enzyme kinetics study of polyamine acetylation by A654L using a fluorescent assay that measures CoA production in the presence of varying amounts of polyamine substrates. Mutation effects of the active site residues Cys-148 or Glu-27 were evaluated using the same enzyme kinetics assay. *Error bars indicate S.D.* *d*, upper panel, structural depiction of the enzyme active site illustrating the key residues Cys-148 and Glu-27 being located adjacent to the cofactor acetyl-CoA. Lower panel, table of enzyme activity of wild-type and mutant proteins. *e*, proposed mechanism of catalysis by A654L.

of the 44 chlorella viruses that have been sequenced (supplemental Fig. 6), Tyr-76 is the only one of the three sites that is conserved in all the viruses, whereas Tyr-79 is a Phe in about half of the viral sequences and Tyr-84 is an Asn in five of the viral vPAT proteins. Therefore, we propose the reaction mechanism (Fig. 2e), which resembles the described catalytic mechanism for lysine acetyltransferases (19).

Polyamines are abundant organic cations with diverse cellular functions whose cellular concentrations are highly regulated (20–23). As efficient inducers of chromatin compaction (24), polyamines are used by some viruses for packaging DNA into viral particles (25, 26). However, the four polyamines detected in the PBCV-1 virion (putrescine, cadaverine, spermidine, and homospermidine) are unlikely to be important in neutralizing its DNA because the number of polyamine molecules per virion could neutralize only ~0.2% of the DNA phosphate residues (5). Presumably, polyamines play an essential role in the PBCV-1 replication cycle because PBCV-1 encodes four functional polyamine biosynthetic enzymes, arginine/ornithine decarboxylase, agmatine iminohydrolase, *N*-carbamoylputrescine amidohydrolase, and homospermidine synthase (HSS) (5, 6, 27). The first three enzymes can convert arginine to putrescine, which is an important intermediate in the synthesis of spermidine, spermine, and homospermidine (supplemental Fig. 7). With the exception of the *hss* gene, all of the genes,

including *vpat*, are expressed prior to initiation of PBCV-1 DNA synthesis (which occurs 60–90 min after PBCV-1 infection), and thus they are classified as early genes. Therefore, one might expect the polyamine levels to increase during the first 60 min of PBCV-1 infection. However, little change occurs in either the polyamine concentration or its composition during the first 60 min of virus infection (5). By 240 min after infection, the concentration of putrescine increases about 3.5 times, whereas the other polyamines decrease during this time. The net result is that the total cellular polyamine concentration decreases slightly during virus replication, possibly due to the action of vPAT. The fact that PBCV-1 encodes enzymes involved in both polyamine biosynthesis and polyamine catalysis suggests that the virus needs to tightly regulate polyamine concentrations in its host during its replication.

In mammalian cells, polyamine acetylation is the first rate-limiting step in polyamine catabolism, and the human acetyltransferase, spermidine/spermine *N*¹-acetyltransferase, is highly regulated due to the association of polyamine abundance with cellular proliferation (19, 20, 28). Through our newly determined crystal structure of vPAT and characterization of its catalytic activity as a polyamine acetyltransferase, we describe for the first time a virally encoded polyamine acetyltransferase with a catalytic efficiency ($K_m = 21 \mu\text{M}$ and $k_{cat} = 131 \text{ min}^{-1}$) that is similar to that of the human spermine

acetyltransferase spermidine/spermine N^1 -acetyltransferase ($K_m = 5.7 \mu\text{M}$ and $k_{\text{cat}} = 155 \text{ min}^{-1}$) (10) and more efficient than that of a bacterial spermine acetyltransferase PaiA ($K_m = 76 \mu\text{M}$ and $k_{\text{cat}} = 19 \text{ min}^{-1}$) (19, 32). Therefore, our study suggests a new basic molecular mechanism by which a eukaryotic virus depletes polyamines in the host, presumably for its own advantage for replication. Support for the importance of vPAT in chlorella virus replication is the finding that the *vpat* gene is present in all 44 of the chlorella viruses that have been sequenced to date (29–31).³

Acknowledgments—We acknowledge the staff at the X6A beamline of the National Synchrotron Light Sources at the Brookhaven National Laboratory for facilitating x-ray data collection. We thank Alexander N. Plotnikov for technical advice and helpful discussion and David Dunigan and Adrian Jeanniard for contributions to the sequencing and annotation of most of the 44 viruses.

REFERENCES

- Wei, H., and Zhou, M. M. (2010) Viral-encoded enzymes that target host chromatin functions. *Biochim. Biophys. Acta* **1799**, 296–301
- de Souza, R. F., Iyer, L. M., and Aravind, L. (2010) Diversity and evolution of chromatin proteins encoded by DNA viruses. *Biochim. Biophys. Acta* **1799**, 302–318
- Kang, M., Moroni, A., Gazzarrini, S., DiFrancesco, D., Thiel, G., Severino, M., and Van Etten, J. L. (2004) Small potassium ion channel proteins encoded by chlorella viruses. *Proc. Natl. Acad. Sci. U.S.A.* **101**, 5318–5324
- Gazzarrini, S., Severino, M., Lombardi, M., Morandi, M., DiFrancesco, D., Van Etten, J. L., Thiel, G., and Moroni, A. (2003) The viral potassium channel Kcv: structural and functional features. *FEBS Lett.* **552**, 12–16
- Kaiser, A., Vollmert, M., Tholl, D., Graves, M. V., Gurnon, J. R., Xing, W., Lisek, A. D., Nickerson, K. W., and Van Etten, J. L. (1999) Chlorella virus PBCV-1 encodes a functional homospermidine synthase. *Virology* **263**, 254–262
- Baumann, S., Sander, A., Gurnon, J. R., Yanai-Balser, G. M., Van Etten, J. L., and Piotrowski, M. (2007) Chlorella viruses contain genes encoding a complete polyamine biosynthetic pathway. *Virology* **360**, 209–217
- Van Etten, J. L., Lane, L. C., and Dunigan, D. D. (2010) DNA viruses: the really big ones (giruses). *Annu. Rev. Microbiol.* **64**, 83–99
- Mujtaba, S., Manzur, K. L., Gurnon, J. R., Kang, M., Van Etten, J. L., and Zhou, M. M. (2008) Epigenetic transcriptional repression of cellular genes by a viral SET protein. *Nat. Cell Biol.* **10**, 1114–1122
- Wei, H., and Zhou, M. M. (2010) Dimerization of a viral SET protein endows its function. *Proc. Natl. Acad. Sci. U.S.A.* **107**, 18433–18438
- Vetting, M. W., S. de Carvalho, L. P., Yu, M., Hegde, S. S., Magnet, S., Roderick, S. L., and Blanchard, J. S. (2005) Structure and functions of the GNAT superfamily of acetyltransferases. *Arch. Biochem. Biophys.* **433**, 212–226
- Dyda, F., Klein, D. C., and Hickman, A. B. (2000) GCN5-related *N*-acetyltransferases: a structural overview. *Annu. Rev. Biophys. Biomol. Struct.* **29**, 81–103
- Jancarik, J., Pufan, R., Hong, C., Kim, S. H., and Kim, R. (2004) Optimum solubility (OS) screening: an efficient method to optimize buffer conditions for homogeneity and crystallization of proteins. *Acta Crystallogr. D Biol. Crystallogr.* **60**, 1670–1673
- Adams, P. D., Grosse-Kunstleve, R. W., Hung, L. W., Ioerger, T. R., McCoy, A. J., Moriarty, N. W., Read, R. J., Sacchettini, J. C., Sauter, N. K., Terwilliger, T. C. (2002) PHENIX: building new software for automated crystallographic structure determination. *Acta Crystallogr. D Biol. Crystallogr.* **58**, 1948–1954
- Emsley, P., and Cowtan, K. (2004) Coot: model-building tools for molecular graphics. *Acta Crystallogr. D Biol. Crystallogr.* **60**, 2126–2132
- Strohalm, M., Kavan, D., Novák, P., Volný, M., and Havlíček, V. (2010) mMass 3: a cross-platform software environment for precise analysis of mass spectrometric data. *Anal. Chem.* **82**, 4648–4651
- Triebel, R. C., Li, F. Y., and Marmorstein, R. (2000) Application of a fluorescent histone acetyltransferase assay to probe the substrate specificity of the human p300/CBP-associated factor. *Anal. Biochem.* **287**, 319–328
- Holm, L., and Rosenström, P. (2010) Dali server: conservation mapping in 3D. *Nucleic Acids Res.* **38**, W545–549
- Benson, L. J., Phillips, J. A., Gu, Y., Parthun, M. R., Hoffman, C. S., and Annunziato, A. T. (2007) Properties of the type B histone acetyltransferase Hat1: H4 tail interaction, site preference, and involvement in DNA repair. *J. Biol. Chem.* **282**, 836–842
- Hegde, S. S., Chandler, J., Vetting, M. W., Yu, M., and Blanchard, J. S. (2007) Mechanistic and structural analysis of human spermidine/spermine N^1 -acetyltransferase. *Biochemistry* **46**, 7187–7195
- Marton, L. J., and Pegg, A. E. (1995) Polyamines as targets for therapeutic intervention. *Annu. Rev. Pharmacol. Toxicol.* **35**, 55–91
- Persson, L. (2009) Polyamine homeostasis. *Essays Biochem.* **46**, 11–24
- Gerner, E. W., and Meyskens, F. L., Jr. (2004) Polyamines and cancer: old molecules, new understanding. *Nat. Rev. Cancer* **4**, 781–792
- Casero, R. A., Jr., and Marton, L. J. (2007) Targeting polyamine metabolism and function in cancer and other hyperproliferative diseases. *Nat. Rev. Drug Discov.* **6**, 373–390
- Sen, D., and Crothers, D. M. (1986) Condensation of chromatin: role of multivalent cations. *Biochemistry* **25**, 1495–1503
- Balint, R., and Cohen, S. S. (1985) The incorporation of radiolabeled polyamines and methionine into turnip yellow mosaic virus in protoplasts from infected plants. *Virology* **144**, 181–193
- Balint, R., and Cohen, S. S. (1985) The effects of dicyclohexylamine on polyamine biosynthesis and incorporation into turnip yellow mosaic virus in Chinese cabbage protoplasts infected *in vitro*. *Virology* **144**, 194–203
- Shah, R., Coleman, C. S., Mir, K., Baldwin, J., Van Etten, J. L., Grishin, N. V., Pegg, A. E., Stanley, B. A., and Phillips, M. A. (2004) *Paramecium bursaria* chlorella virus-1 encodes an unusual arginine decarboxylase that is a close homolog of eukaryotic ornithine decarboxylases. *J. Biol. Chem.* **279**, 35760–35767
- Babbar, N., Hacker, A., Huang, Y., and Casero, R. A., Jr. (2006) Tumor necrosis factor α induces spermidine/spermine N^1 -acetyltransferase through nuclear factor κB in non-small cell lung cancer cells. *J. Biol. Chem.* **281**, 24182–24192
- Fitzgerald, L. A., Graves, M. V., Li, X., Feldblyum, T., Hartigan, J., and Van Etten, J. L. (2007) Sequence and annotation of the 314-kb MT325 and the 321-kb FR483 viruses that infect *Chlorella* Pbi. *Virology* **358**, 459–471
- Fitzgerald, L. A., Graves, M. V., Li, X., Feldblyum, T., Nierman, W. C., and Van Etten, J. L. (2007) Sequence and annotation of the 369-kb NY-2A and the 345-kb AR158 viruses that infect *Chlorella* NC64A. *Virology* **358**, 472–484
- Fitzgerald, L. A., Graves, M. V., Li, X., Hartigan, J., Pfitzner, A. J., Hoffart, E., and Van Etten, J. L. (2007) Sequence and annotation of the 288-kb ATCV-1 virus that infects an endosymbiotic chlorella strain of the heliozoon *Acanthocystis turfacea*. *Virology* **362**, 350–361
- Forouhar, F., Lee, I. S., Vujcic, J., Vujcic, S., Shen, J., Vorobiev, S. M., Xiao, R., Acton, T. B., Montelione, G. T., Porter, C. W., and Tong, L. (2005) Structural and functional evidence for *Bacillus subtilis* PaiA as a novel N^1 -spermidine/spermine acetyltransferase. *J. Biol. Chem.* **280**, 40328–40336

³ J. L. Van Etten, unpublished results.

Supplemental Materials And Methods

Zachary Charlop-Powers et al.

Reagents

All chemical reagents unless otherwise noted were obtained from Sigma Aldrich. All restriction enzymes and polymerases were purchased from New England Biolabs.

Molecular Cloning

The *A654L* gene was cloned from the PBCV-1 genome by PCR using primers incorporating NdeI and BglIII restriction sites. The forward and reverse primers are 5'-ATTTCAACATATGTA TACGCTAATCAAAC-3', and 5'-AAAGAGATCTCTAAATAGTTTTGACCATAC-3', respectively. The PCR fragment was digested and ligated to pre-digested pET-15b vector (Novagen) that encodes a recombinant protein with a N-terminal polyhistidine tag.

Mutagenesis

Point mutations of A654L residues Cys148 and Glu27 to Ala and Gln, respectively, were generated with designed primers obtained from IDTDNA. Using PFU polymerase and a 3-step thermocycling program (95, 55, 65 at 30sec, 30sec, 8min) for 20 cycles we generated nicked mutation-containing plasmids. 1 μ L of *DpnI* was added to PCR reactions and incubated for 1 h at 37°C. Mutations were verified by sequencing. The sequences of the primers used in mutagenesis are listed below: (1) C148A, forward primer: 5'-GTATATTTACGGGGATGCCACG-AATATCATCTCGC-3', and reverse primer: 5'-GCGAGATGATATTCGTGGCATCCCCGTAAT-ATAC-3'; and (2) E27Q, forward primer: 5'-GAAATTTTGTGGCGTCACAGCCCACGTCAATTG-C-3', and reverse primer: 5'-GCAATTGACGTGGGCTGTGACGCCACAAAATTC-3'.

Protein Expression and Purification

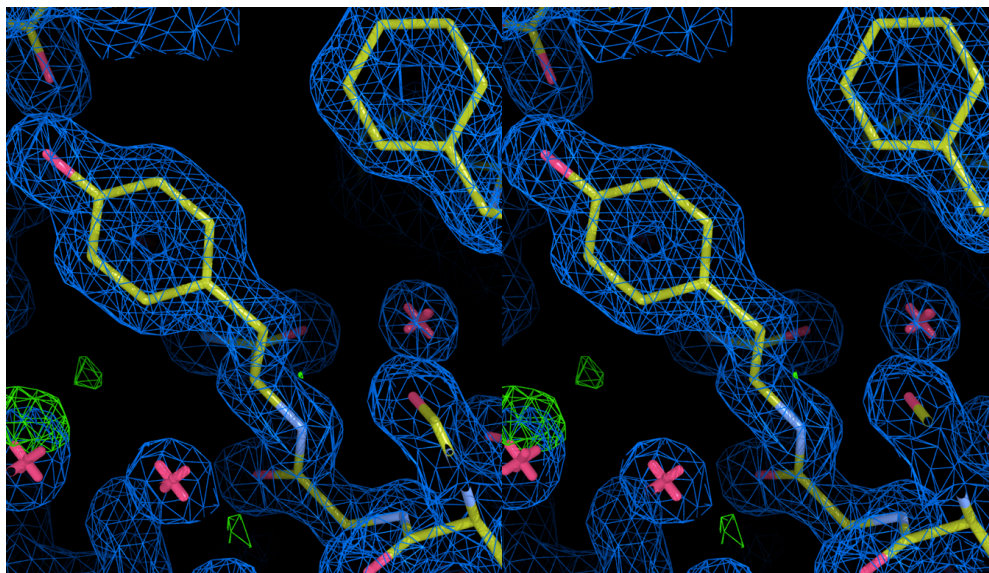
The pET15b-A654L plasmid was transformed into BL21(DE3) cells. Cells were grown in TB media at 37°C until their optical density reached 1.0. The culture was then changed to 18°C and protein expression was induced by the addition of 0.4 mM IPTG. Cells were harvested after 16 hours, washed with PBS buffer of pH 7.4 containing 100 mM sodium chloride and 50 mM sodium phosphate, re-suspended, and homogenized in an ice-cold lysis buffer of 100 mM NaCl, 1 mM EDTA, 10 mM DTT, and 0.5% NP-40. Cells were lysed using a microfluidizer at 18,000 PSI. The polyhistidine-tagged A654L protein was purified using a Nickel-NTA column (GE Healthcare), and followed by a Superdex 75 column in a 20 mM Tris buffer of pH 8.5 containing 200 mM NaCl. After histidine-tag cleavage by thrombin, the protein was further purified using a Source Q column in 20 mM Tris buffer of pH 8.5 with a salt gradient of 0-1 M NaCl.

Supplementary Table 1.
Kinetic Parameters for Acetyl-Coenzyme A and Polyamines

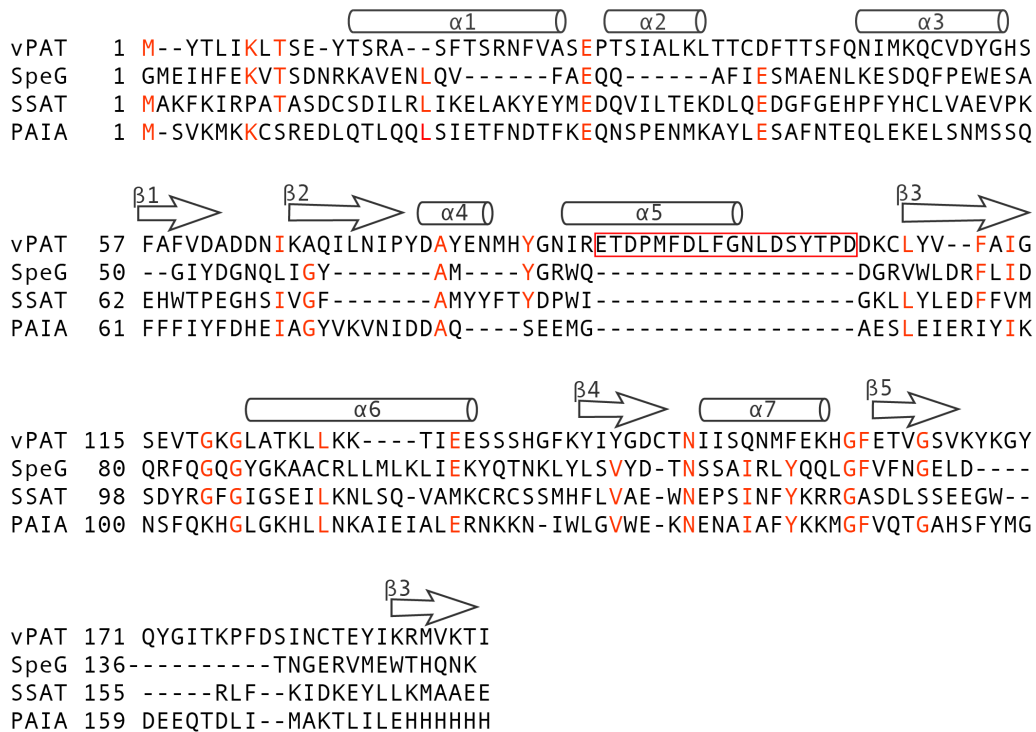
	K_m (μM)	k_{cat} (min^{-1})	k_{cat}/K_m ($\text{M}^{-1}\text{s}^{-1}$)
Acetyl-CoA ^a	4 ± 0.7	138 ± 5.4	608 × 10 ³
Spermine ^b	21 ± 2.4	83.5 ± 1.0	65 × 10 ³
Spermidine ^b	3,423 ± 474	178.1 ± 16.0	0.86 × 10 ³
Putrescine ^b	4,559 ± 1,324	45.0 ± 9.1	0.16 × 10 ³
Cadaverine ^b	135 ± 25	87.3 ± 4.1	11 × 10 ³
Homospermidine ^b	848 ± 157	105.4 ± 8.2	2 × 10 ³

^a Measured at saturating concentration of spermine.

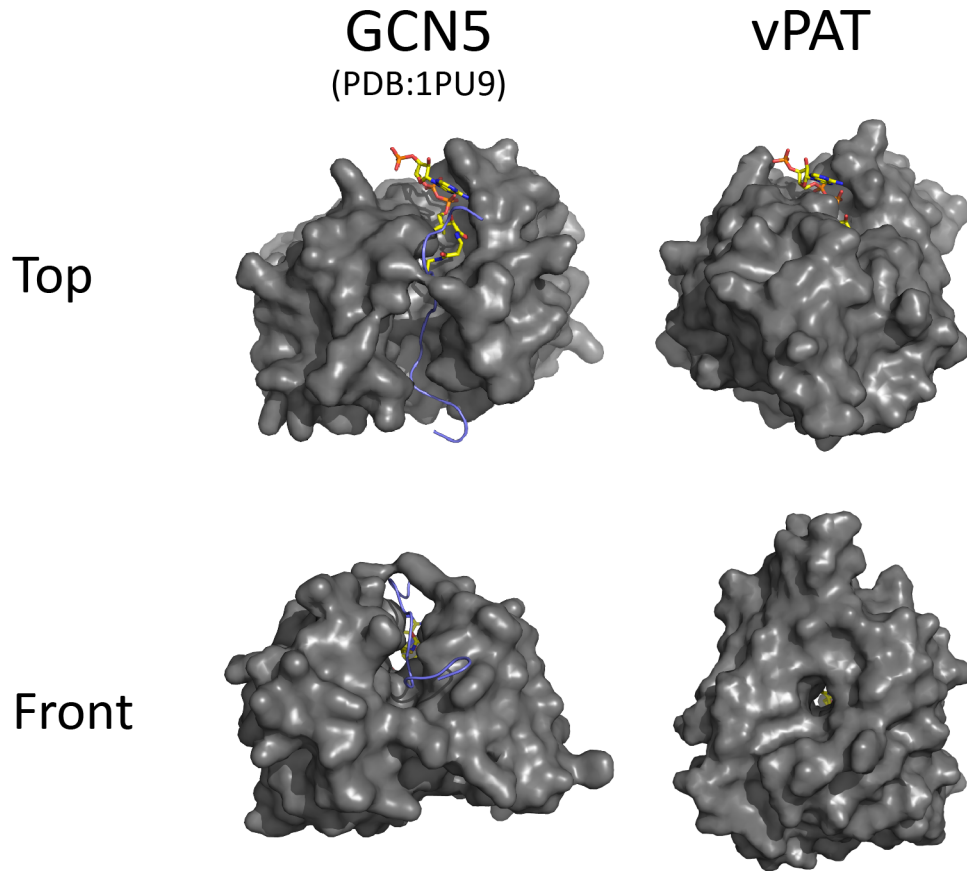
^b Measured at saturating concentration of acetyl-CoA.



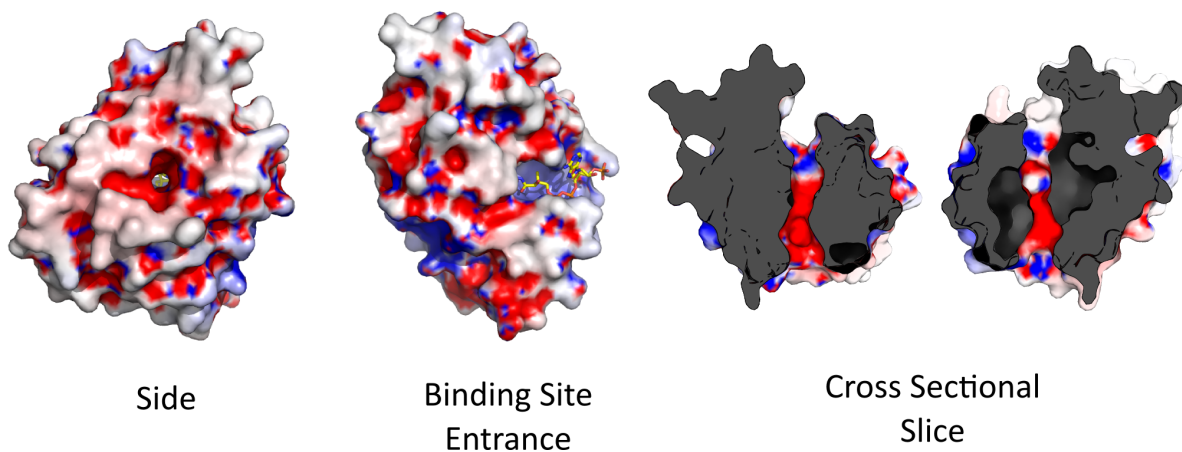
Supplementary Figure 1. Crystal structure of vPAT (A654L). Stereo view of the $2F_o - F_c$ electron density map of the crystal structure of vPAT (A654L) contoured at 1σ .



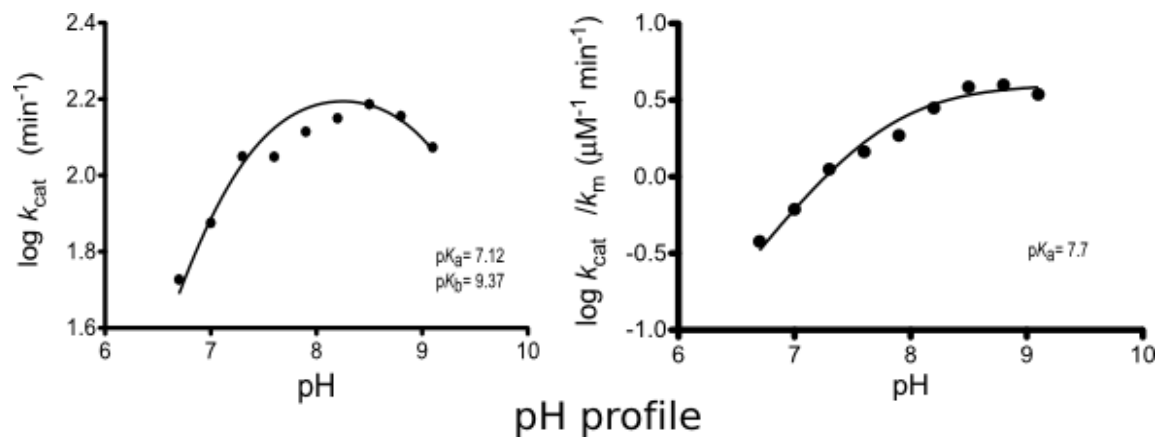
Supplementary Figure 2. Structure-based sequence alignment of acetyltransferases. vPAT (A654L) is listed at the top along with a human (SSAT) and two bacterial (SpeG, *E. faecalis*; PAIA, *B. subtilis*) spermine acetyltransferases. The conserved residues including Glu27 in vPAT (A654L) are colored in red and the unique insert of $\alpha 5$ in vPAT (A654L) is highlighted by a red box.



Supplementary Figure 3. Structural comparison of vPAT (A654L) with *Tetrahymena* GCN5/H3 peptide complex. The GCN5 family histone acetyltransferases have the same fold as vPAT (A654L) but differ in the substrate binding site. The presence of a conserved insert in vPAT (A654L) results in the occlusion of space where the incoming substrate peptide would sit. The result is a narrow water-filled channel extending through vPAT (A654L) (bottom right).



Supplementary Figure 4. Electrostatic surface representation of vPAT (A654L). Mapping of electrostatic potential onto vPAT (A654L) shows a largely negative surface. The cross section of vPAT (A654L) (right) reveals the negatively charged tunnel, suggesting a narrow, cationic substrate.



Supplementary Figure 5. pH-dependent spermine acetylation by vPAT (A654L). The activity of vPAT (A654L) at different pHs was obtained using spermine as a variable substrate. The curves were fit using the equations described in the Supplemental Methods, and the results indicate two residues within the enzyme active site of vPAT (A654L) with pK values important for catalysis.

Supplementary Figure 6. Comparison of vPAT (encoded by PBCV-1) amino acid sequence to those from 44 viruses that infect *Chlorella* species.

Viruses	Sequences	
PBCV-1	MYTLIKLTSEYTSRAISFTSRNFVASEPTSIALKLTTCDFTTSFQNIKQCVDYGHSAFAF	60
CVG-1	---MFKLALKDVS CAMAFTARTFVQAQEPSVALKFTTCDFVTSFADVMTKSIASGLSFAV	57
Fr5L	---MFKLTLKDVSRAMAFTARTFVQAQEPSVALKFTTCDFVTSFADVMTKSIASGLSFAV	57
CZ-2	---MFKLTLKDVSRAMAFTARTFVQAQEPSVALKFTTCDFVTSFADVMTKSIKSGLSFAV	57
OR0704.2.2	---MFKLALKDVS RAMAFTARTFVQAQEPSVALKFTTCDFVTSFADVMTKSIASGLSFAV	57
NW665.2	MIQMFKLTLKDVSRAMAFTARTFVQAQEPSVALKFTTCDFVTSFADVMTKSISSGLSFAV	60
MT325	MIQMFKLTLKDVSRAMAFTARTFVQAQEPSVALKFTTCDFVTSFADVMTKSIASGLSFAV	60
Can18-4	MIQMFKLALKDVPRAMAFTARTFVQAQEPSVALKFTTCDFVTSFADVMTKSIASGLSFAV	60
CVR-1	---MFKLALKDVPRAMAFTARTFVQAQEPSVALKFTTCDFVTSFADVMTKSIASGLSFAV	57
AP110A	---MFKLALKDVPRAMAFTARTFVQAQEPSVALKFTTCDFVTSFADVMTKSIASGLSFAV	57
CVM-1	---MFKLALKDVH RAMAFTARTFVQAQEPSVALKFTTCDFVTSFADVMTKSIASGLSFAV	57
FR483	MIKMFKLALKDVPRAMAFTARTFVQAQEPSVALKFTTCDFVTSFADVMTKSIASGLSFAV	60
CVB-1	---MFKLALKDVSRAMAFTARTFVQAQEPSVALKFTTCDFVTSFADVMTKSIASGLSFAV	57
NE-JV-1	---MFRLASKDLPRAMAFTARTFVASEPTSVALKLTTCDFVTAQDVMQKAVESGYSFAH	57
CVA-1	---MFRLASKDLPRAMAFTARTFVASEPTSVALKLTTCDFVTAQDVMQKAVESGYSFAH	57
ATCV-1	---MYMLRLTPSHISKAIQFTSRFTFVKAEPSVALKFTTCDFTTAFQDVMKKCIESGYSFAH	59
OR0704.3	---MYMLRLTPSHISKAIQFTSRFTFVKAEPSVALKFTTCDFTTAFQDVMKKCIESGYSFAH	59
NE-JV-3	---MYMLRLTPSHISKAIQFTSRFTFVKAEPSVALKFTTCDFTTAFQDVMKKCIESGYSFAH	59
Can06105P	---MYMLRLTPNHINKAIQFTSRFTFVKAEPSVALKFTTCDFTTAFQDVMKKCIESGYSFAH	59
WI0606	---MYMLRLTPSHISKAIQFASRTFVKAEPSVALKFTTCDFTTAFQDVMKKCIESGYSFAH	59
MO0605SPH	---MYMLRLTPSHISKAIQFASRTFVKAEPSVALKFTTCDFTTAFQDVMKKCIESGYSFAH	59
NE-JV-2	---MLRLTPSHVSKAIQFTSRFTFVKAEPSVALKFTTCDFTTAFQDVMKKCIESGYSFAH	57
TN603.4.2	---MLRLTPSYVSKAIQFTSRFTFVRAEPSVALNFTTCDFTTAFQDVMKRCVDSGYSFAH	57
GM0701.1	---MLRLTPSYVSKAIQFTSRFTFVRAEPSVALNFTTCDFTTAFQDVMKRCVDSGYSFAH	57
Br0604L	---MLRLTSSHLSKAIQFTSRFTFVRAEPSVALKFTTCDFTTAFQDVMKRCVDSGYSFAH	57
Smith-1	---MFRLTLNHASKAIQFTSRFTFVKAEPSVALNFTTCDFTTAFQDVMKRCVDSGYSFAH	57
MN0810.1	---MLRLAHIHASKAIQFTTRFTFIKAEPSVALNFTTCDFATAFQDVMKRCVDSGYSFAH	57
NTS-1	---MLRLTPSHVSKAIQFTSRFSVKAEPSVALKFTTCDFTTAFQDVMKKCIDSGYSFAH	57
Perrin-052	---MIRLTTGHVRKAIQFTSRFSVKAEPSVALKFTTCDFTTAFQDVMKRCVDSGYSFAH	57
Canal-1	---MIRLTTGHVRKAIQFTSRFSVKAEPSVALKFTTCDFTTAFQDVMKRCVDSGYSFAH	57
CME6	MYTLIKLTSEYTSRAISFTSRNFVASEPTSIALKLTTCDFTTSFQNIKQCVDYGHSAFAF	60
CviKI	MYTLIKLTSEYTSRAISFTSRNFVASEPTSIALKLTTCDFTTSFQNIKQCVDYGHSAFAF	60
NE-JV-4	MYTLIKLTSEYTSRAISFTSRNFVASEPTSIALKLTTCDFTTSFQNIKQCVDYGHSAFAF	60
AN69C	MYTLIKLTSEYTARAI SFTSRNFVASEPTSIALKLTTCDFTTSFQNIKQCVDYGHSAFAF	60
IL-3A	MYTLIKLTSEYTARAI SFTSRNFVASEPTSIALKLTTCDFTTSFQNIKQCVDYGHSAFAF	60
MA-1E	MYTLIKLTSEYTARAI SFTSRNFVASEPTSIALKLTTCDFTTSFQNIKQCVDYGHSAFAF	60
CvsAI	MYTLIKLTSEYTARAI SFTSRNFVASEPTSIALKLTTCDFTTSFQNIKQCVDYGHSAFAF	60
NY-2B	MYTLIKLTSEYTSRAIAFASKNFTTSEPTSIALKLTTCDFTTSFQNIKQCVDEHDHSAFAF	60
MA-1D	MYTLIKLTSEYTSRAIAFASKNFTTSEPTSIALKLTTCDFTTSFQNIKQCVDEHDHSAFAF	60
NYS-1	MYTLIKLTSEYTYRAIAFASKNFTTSEPTSIALKLTTCDFTTSFQNIKQCVDEHDHSAFAF	60
IL-5-2s1	MYTLIKLTSEYTYRAIAFASKNFTTSEPTSIALKLTTCDFTTSFQNIKQCVDEHDHSAFAF	60
AR158	MCTLIKLTSEYTSRAIAFASKNFTTSEPTSIALKLTTCDFTTSFQNIKQCVDEHDHSAFAF	60
NY-2A	MYTLIKLTSEYTSRAITFASKNFTTSEPTSVALKLTTCDFTTSFQNIKQCVDEHNHSAFAF	60
KS-1B	MYELIRLTSYIPRAISFTSRNFVASEPTSVALKLTTCDFTTSFQNIKHCVESGYSFAF	60
	::::: *: *:::.* *****:::***** *: * ::* ::: . ***	

Viruses

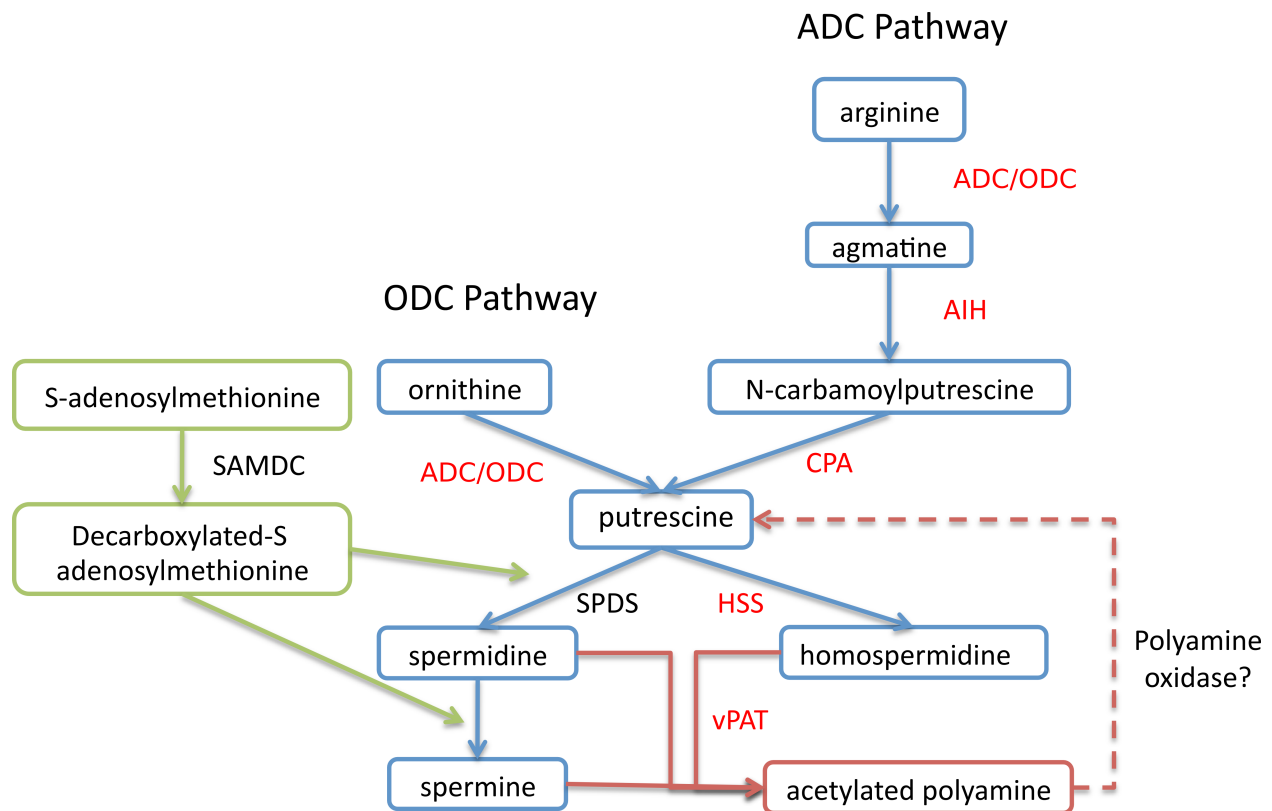
Sequences

PBCV-1	VDADDNIKAQILNIPYDAYENMHYGNIRETDPMFDFLGNLDSYTPDDKCLYVFAIGSEVT	120
CVG-1	EDDNGDIVAQSLSIDYDTFVMANYGHTRESAPMFDFLFSKLDAYVVPNKCVVVFALISSEVQ	117
Fr5L	EDDNGDIVAQSLSIDYDTFVMANYGHTRESAPMFDFLFSKLDAYVVPNKCVVVFALISSEVQ	117
CZ-2	EDENGDIVAQSLSIDYDTFVMANYGHTRESAPMFDFLFSKLDAYVVPNKCVVVFALISSEVQ	117
OR0704.2.2	EDENGDIVAQSLSIDYDTFVMANYGHTRESAPMFDFLFSKLDAYVVPNKCVVVFALISSEVQ	117
NW665.2	EDDNGDIVAQSLSIDYDTFAMANYGHTRESAPMFDFLFSKLDAYVVPNKCVVVFALISSEVQ	120
MT325	EDDNGDIVAQSLSIDYDTFVMANYGHTRESAPMFDFLFSKLDAYVVPNKCVVVFALISSEVQ	120
Can18-4	EDDNGDIVAQSLSIDYDTFVMANYGHTRESAPMFDFLFSKLDAYVVPNKCVVVFALISSEVQ	120
CVR-1	EDDNGDIVAQSLSIDYNTFTMANYGHTRESAPMFDFLFSKLDAYVVPNKCVVVFALISSEVQ	117
AP110A	EDDNGDIVAQSLSIDYNTFTMANYGHTRESAPMFDFLFSKLDAYVVPNKCVVVFALISSEVQ	117
CVM-1	EDDNGDIVAQSLSIDYNTFTMANYGHTRESAPMFDFLFSKLDAYVVPNKCVVVFALISSEVQ	117
FR483	EDDNGDIVAQSLSIDYDTFAVANYGHTRESAPMFDFLFSKLDAYVVPNKCVVVFALISSEVQ	120
CVB-1	EDDNGDIVAQSLSIDYDTFAMANYGHTRESAPMFDFLFSKLDAYVVPNKCVVVFALISSEVQ	117
NE-JV-1	ENEQKNIVAQSLSVPYATFASANYGHTRETAPMFDFLFSHLDSEPHENTIVVFAISSEIK	117
CVA-1	ENEQKNIVAQSLSVPYATFASANYGHTRETAPMFDFLFSHLDSEPHENTIVVFAISSEIK	117
ATCV-1	ME-NGEIVAQSLTVPYAMFTAANYGYTRETQPMFDFLSELEAYTPERKCLVVFALSSEVE	118
OR0704.3	ME-NGEIVAQSLTVPYDMFTAANYGYTRETQPMFDFLSELEAYTPERKCLVVFALSSEVE	118
NE-JV-3	ME-NGEIVAQSLTVPYDMFTAANYGYTRETQPMFDFLSELEAYTPERKCLVVFALSSEVE	118
Can06105P	ME-NGEIVAQSLTVPYDMFTAANYGYTRETQPMFDFLSELEAYTPERKCLVAFALSSEVE	118
WI0606	ME-NGEIVAQSLTVPYDIFTSANYGYTRETQPMFDFLSELEAYTPERKCLVVFALSSEVE	118
MO0605SPH	ME-NGEIVAQSLTVPYDIFTSANYGYTRETQPMFDFLSELEAYTPERKCLVVFALSSEVE	118
NE-JV-2	ME-NGEIVAQSLTVPYDIFTSANYGYTRETQPVDFLSELEVYTPPEAKCLVVFALSSEVE	116
TN603.4.2	ME-NGEIVAQSLTVPYDIFMQANNGHRTETPEMFDFLFSKLDYTPKEKCLVVFALSSEVE	116
GM0701.1	ME-NGEIVAQSLTVPYDIFMQANNGHRTETPEMFDFLFSKLDYTPKEKCLVVFALSSEVE	116
Br0604L	ME-NGEIVAQSLTVPYDIFMQANNGHRTETPEMFDFLSTLDYTPKEKCLVVFALSSEVE	116
Smith-1	ME-NGEIVAQSLTVPYDKFTTANYGYTRETQPMFDFLSELEVYTPKEKCLVVFALSSEVE	116
MN0810.1	ME-NGEIVAQSLTVPYDKFMAANYGYTRETQPMFDFLSELEIYEPKEKCLVVFALSSEVE	116
NTS-1	ME-NGEIVAQSLTVPYDIFMAANYGYTRETQPMFDFLSELEAYEPRKCLVVFALSSEVE	116
Perrin-052	LE-DDKIVAQSLAVPYDIFMTANNGHRTETPEMFDFLSELDVYEPRKCLVMFALSSEVE	116
Canal-1	LE-DDKIVAQSLAVPYDIFMTANNGHRTETPEMFDFLSELDVYEPRKCLVMFALSSEVE	116
CME6	VDADDNIKAQILNIPYDAYENMHYGNIRETDPMFDFLGNLDSYTPDDKCLYVFAIGSEVT	120
CvIKI	VDADDNIKAQILNIPYDAYENMHYGNIRETDPMFDFLGNLDSYTPDDKCLYVFAIGSEVT	120
NE-JV-4	VDADDNIKAQILNIPYDAYENMHYGNIRETDPMFDFLGNLDSYTPDDKCLYVFAIGSEVT	120
AN69C	VDADDNIKAQILNIPYDAYENMHYGNIRETDPMFDFLGNLDSYTPDDKCLYVFAIGSEVT	120
IL-3A	VDADDNIKAQILNIPYDAYENMHYGNIRETDPMFDFLGNLDSYTPDDKCLYVFAIGSEVT	120
MA-1E	VDADDNIKAQILNIPYDAYENMHYGNIRETDPMFDFLGNLDFYTPDDKCLYVFAIGSEVT	120
CvsAI	VDADDNIKAQILNIPYDAYENMHYGNIRETDPMFDFLGNLDFYTPDDKCLYVFAIGSEVT	120
NY-2B	VDANDNIKAQILNIPYEYYENMHYGNIRETDPMFDFLGNLDVYTPNDKCLYVFAIGSEDS	120
MA-1D	VDANDNIKAQILNIPYEYYENMHYGNIRETDPMFDFLGNLDVYTPNDKCLYVFAIGSEDS	120
NYS-1	VDANDNIKAQILNIPYEYYENMHYGNIRETDPMFDFLGNLDVYTPNDKCLYVFAIGSEDS	120
IL-5-2s1	VDANDNIKAQILNIPYEYYENMHYGNIRETDPMFDFLGNLDVYTPNDKCLYVFAIGSEDS	120
AR158	VDANDNIKAQILNIPYEYYENMHYGNIRETDPMFDFLGNLDVYTPNDKCLYVFAIGSEDS	120
NY-2A	VDAHDNIKAQILNIPYEAYENVHYGNIRETDPMFDFLGNLDVYTPNDKCMYVFAIGSEVT	120
KS-1B	VDTNDNIKAQILNIPYDVYENMHYGNIRETDPMFDFLGNLDSYAPDDKCMYVFAIGSEVT	120
	: . . * * * * : * : : * ** : * : * * * . * : * * . : ** : . **	

Viruses

Sequences

PBCV-1	FDSINCTEYIKRMVKTI-	197
CVG-1	YASINDTKGIQRMILNI-	194
Fr5L	YASINDTKGIQRMILNI-	194
CZ-2	YACINDTQGIQRMILNI-	194
OR0704.2.2	YACINDTQGIQRMILNI-	194
NW665.2	YACINDTRGIQRMILNI-	197
MT325	YASINDTRGIQRMILNI-	197
Can18-4	YASINDTRGIQRMILNI-	197
CVR-1	YACINDTRGIQRMVLHI-	194
AP110A	YACINDTRGIQRMVLHI-	194
CVM-1	YACINDTRGIQRMVLHI-	194
FR483	YACINDTRGIQRMVLHI-	197
CVB-1	YACINDTRGIQRMVLHI-	194
NE-JV-1	FESIVDTRGIQRMTLSV	195
CVA-1	FESIVDTRGIQRMTLSV	195
ATCV-1	FKSIKCTNDVQRMVLEL-	195
OR0704.3	FKSIKCTNDVQRMVLEL-	195
NE-JV-3	FKSIKCTNDVQRMVLEL-	195
Can06105P	FKSIKCTNDVQRMVLEL-	195
WI0606	FKSIKCTNDVQRMVLEL-	195
MO0605SPH	FKSITCTNDVQRMVLEL-	195
NE-JV-2	FKSIKCTNDVQRMVLEL-	193
TN603.4.2	FKSIKCTDDVQRMVLKM-	193
GM0701.1	FKSIKCTNDVQRMVLKM-	193
Br0604L	FKSIKCTNDVQRMVLKM-	193
Smith-1	FRSIKDTKNVQRMVLKV-	193
MN0810.1	FKSIKDTKDVQRMVLKV-	193
NTS-1	FKSIKDTKDVQRMVLCL-	193
Perrin-052	FKSIRGTDDVKRMVLEL-	193
Canal-1	FKSIRGTDDVKRMVLEL-	193
CME6	FDSINCTEYIKRMVKTI-	197
CvIKI	FDSINCTEYIKRMVKTI-	197
NE-JV-4	FDSINCTEYIKRMVKTI-	197
AN69C	FDSINCTEYIKRMVKTI-	197
IL-3A	FDSINCTEYIKRMVKTI-	197
MA-1E	FDSINCTEYIKRMVKTI-	197
CvsAI	FDSINCTEYIKRMVKTI-	197
NY-2B	FDSINCTEYIKRMVKTM-	197
MA-1D	FDSINCTEYIKRMVKTM-	197
NYS-1	FDSINCTEYIKRMVKTM-	197
IL-5-2s1	FDSINCTEYIKRMVKTM-	197
AR158	FDSINCTEYIKRMVKTM-	197
NY-2A	FDSINCTEYIKRMVKTM-	197
KS-1B	FDSINCTESIKRMVKTI-	197
	: .* * :::** :	



Supplementary Figure 7. PBCV1 encodes four enzymes for the biosynthesis of polyamines and at least one for their degradation, highlighted in red in the pathway. The presence of arginine/ornithine decarboxylase (ADC/ODC), agmatine iminohydrolase (AIH), N-carbamoylputrescine amidohydrolase (CPA), and homospermidine synthase (HSS) are previously characterized enzymes allowing for the biosynthesis of homospermidine from arginine. In this study, we demonstrate that PBCV1 also encodes an enzyme, vPAT (A654L), capable of acetylating polyamines, which is the first step in degradation usually followed by oxidation through a polyamine oxidase. Note that genes encoding enzymes ADC/ODC, AIH, CPA and vPAT are expressed prior to the initiation of viral DNA synthesis and thus are classified as early genes. The gene encoding HSS is expressed after initiation of viral DNA synthesis and is classified as a late gene. HSS is the only one of the 5 proteins that is packaged in the virion (JVE, unpublished results).